

Preparation of poly (N-imidazolylmaleamic acid) /nanomaterial coating films on stainless steel by electrochemical polymerization to study the anticorrosion and antibacterial action

Khulood A. Saleh, Khalil S. Khalil, Muna I. Khalaf

Department of Chemistry, College of science, University of Baghdad, Baghdad, Iraq.
Corresponding Author: Khulooda.Saleh

Abstract: Poly (N-Imidazolylmaleamic acid) PIM was synthesized from monomer (N-Imidazolylmaleamic acid) NIM in aqueous solution using electrochemical oxidation procedures. The polymer film was formed on stainless steel electrodes (working electrode). Its structure has been examined by infrared, FTIR, scanning electron microscopy SEM and atomic force microscopy AFM studies indicate that the polymer was formed. Also, study the anticorrosion action of polymer film on stainless steel by electrochemical polarization method. Furthermore, enhanced the anticorrosion of polymer by nanomaterial such as (TiO₂ and ZnO (bulk-nano)) by adding to monomer solution. The results obtained showed that the corrosion rate of S-steel increased with temperature increase from 293K to 323K and the values of inhibition efficiency by coating polymer increase with nanomaterial addition. Kinetic and thermodynamic of activation parameters have been calculated for the corrosion process of S-steel in acidic medium before and after polymeric coating. Furthermore were studied the effect of the preparing polymer on some strain of bacteria.

Keyword: electro polymerization, N-Imidazolylmaleamic acid, anti-corrosion, nanomaterial.

Date of Submission: 05-01-2018

Date of acceptance: 29-01-2018

I. Introduction

Electrodes coated with polymer films have been the subject of considerable interest in recent years [1]. An especially important class of polymers in this respect are electronically conducting polymers such as poly (N-Imidazolylmaleamic acid) or PIM. A common method to obtain thin films of conducting polymers is the electrochemical polymerization of the corresponding monomers from electrolyte solutions [2-4]. The flow of an electric current through a monomer solution may allow for (1) the growth of a polymer film on the electrode surface [5-6] (2) monomer polymerization in solution [7- 8] or (3) irreversible monomer oxidation or reduction to non-polymeric products. The reaction path followed by a specific monomer depends on the nature of the electrode, the background electrolyte, the solvent, and the working conditions. Electrochemically initiated polymer production may become an alternative method with many possibilities as continuous process, if it were possible to control the polymerization rate, monomer conversion, and the molecular weight distribution by monitoring the chemical and electrochemical parameters (concentration, temperature, electrode material, electrode activation, current densities, or potential of polymerization). The grafting of polymer chains onto solid substrates is of major interest for the design of materials with specific surface and structural properties. These modified materials are of technological interest. For instance, substrates coated with polymer films have great potential for applications in the medical domain [9]. The formation of a dense and homogeneous distribution of chemical bonds between the substrate and the polymer would resist mechanical stress and chemical attack from the environment and oppose microbial colonization. Recently, we have shown that the application of an anodic potential to a solution of NIM leads to the grafting and polymerization of the monomer onto S-steel electrodes [10-13]. Infrared FTIR reflection-absorption spectroscopies, SEM and AFM have revealed the presence of thin PIM films on this surface. Corrosion inhibitors are widely used in industry to reduce the corrosion rate of metals and alloys in contact with aggressive environment [14–17]. In this paper, electrochemical polarization technique was employed to study the inhibition capability of the polymeric film on the corrosion of S-steel in 0.2M HCl. The effect of temperature is also reported. In addition, we study the influence of adding different nanomaterial compound such as (TiO₂ and ZnO (bulk-nano)) on the anticorrosion action of polymer on S-steel surface.

II. Experimental

The electrochemical polymerization of NIM onto the S-steel (anode) electrode surface was carried out in a potentiostat using a regulated DC power supply. The electrodes were cleaned and washed by acetone. The solutions employed for polymerization were 0.1g of N-imidazole maleamic acid (monomer) [18] in 100ml H₂O

with three drop of H₂SO₄ concentration (37%). The polymerization was carried out at 2V and at 293K. The polymer film was deposited at the anode surface.

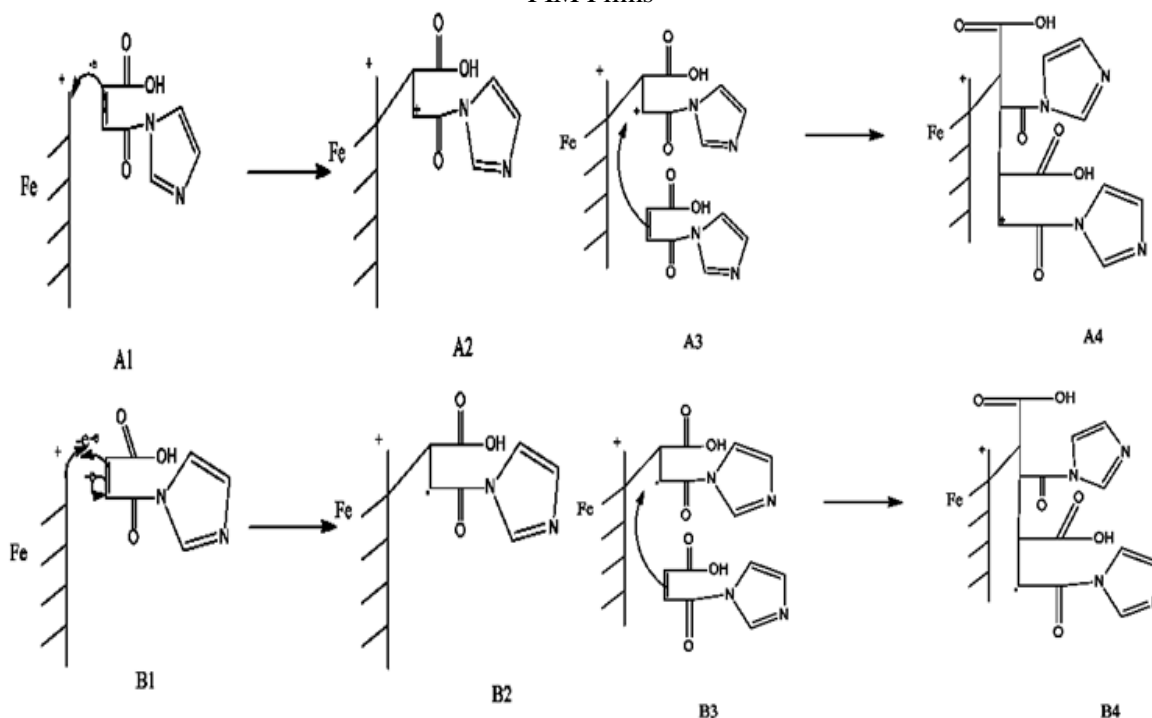
For corrosion measurements, Stainless steel was used for the study. The sheet was mechanically press-cut to form coupons, each of dimension, 3x2 cm. Each coupon was degreased by washing with ethanol. The washed sample was dipped in acetone removed and allowed to dry in air before use. A platinum was used as auxiliary electrode and a saturated calomel electrode (SCE) as reference electrode, stainless steel was used as the working electrode. Anodic and cathodic polarization of S-steel was carried out under potentiostatic conditions in 0.2M HCl in the absence as well as in the presence-coated layer, all the experiments were carried out at different temperature (293-323) K. Also, in presence of 0.05g of ZnO (bulk-nano) and TiO₂nanomaterial which add to improve the coated layer against corrosion and bacteria.

III. Result and discussion

3.1.Mechanism of Polymerization

Based on the published literature, a cationic [19-20]or a radical mechanism [21-25] can be proposed to explain electro polymerization reactions and, in particular, the grafting and the growth of the PIM films. The first consider is the cationic mechanism (Scheme 1A): the application of an anodic potential to an NIM solution implies the transfer of one electron from the monomer to the working electrode (A1). This transfer leads to the formation of a radical cation adsorbed on the electrode surface which is represented in A2. Alternatively, if the lifetime of A2 is long enough compared to the mean time for a NIM molecule to diffuse toward the electrode, then the NIM molecules can add on via a cationic mechanism at the charged ends of the adsorbed oxidized NIM (A4). This process by propagation leads to the formation of a grafted polymer. Let us now consider a radical mechanism [26] (Scheme 1B). The radical counterpart of A2 is B2. First, the chemisorbed radical depicted in B2 cannot be the result of an electrochemical process. If we assume that the grafting step is disconnected from the electrochemical process, we are nevertheless faced with the fact that the radical mechanism is not particularly favored under the present electrochemical conditions. Indeed, the radical mechanism proceeds via a homolytic scission of the double bond (Scheme 1B). However, homolytic rupture of the C=C bond is highly improbable considering the initial polarization of the bond which is further enhanced under the field created by the electric double layer [27]. Moreover, this electric field induces a reorientation of the molecule [28]. This all together makes the radical mechanism rather unlikely to account for the grafting and the growth of PIM films under anodic electrochemical conditions.

Scheme 1. Proposed Cationic (A) and Radical (B) Mechanisms for the Grafting and the Growth of PIM Films



3.2. Structure of PCM

FTIR spectra of PIM coating film prepared from NIM are shown in Fig.2. In this spectra, the characteristic bands of the NIM Fig.1 double bond $C=C$ 1593Cm^{-1} are disappear and confirm the formation of PIM. The bands are relatively broad mainly because the polymer has a broad chain length distribution.

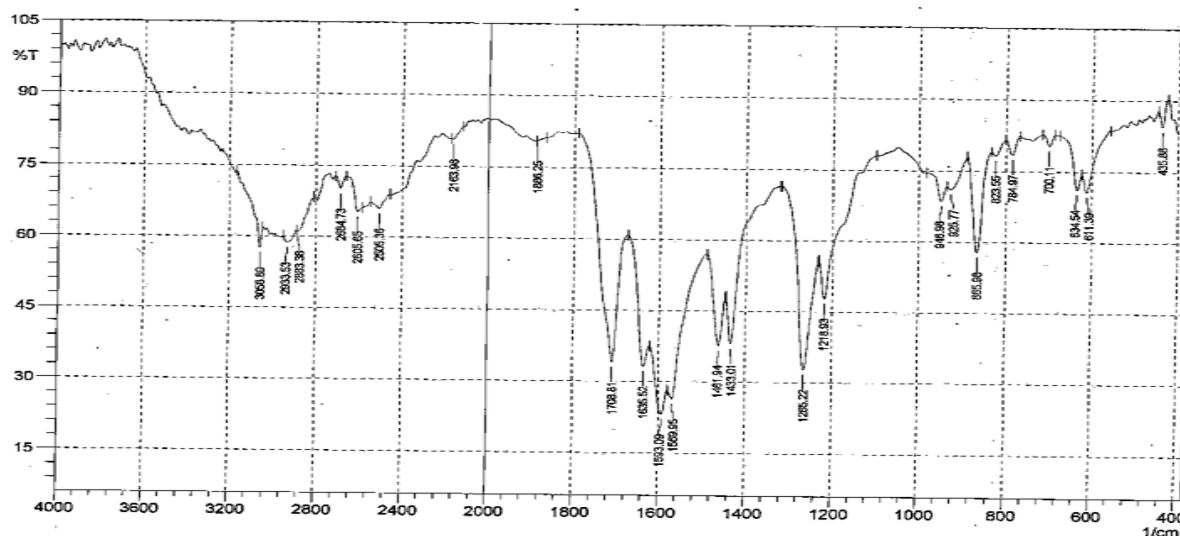


Fig. 1. FTIR spectra of NIM

The band appeared at 1712Cm^{-1} that confirmed the presence of $C=O$ carboxyl groups, the absorption of imide group was appeared at 1647Cm^{-1} , the absorption bonds of $O-H$ carboxylic group appeared at $2700-3300\text{Cm}^{-1}$ [29-31].

3.3. Potentiostatic polarization measurements

The effect of polymeric coating film on the anodic and cathodic polarization curves of S-steel in 0.2M HCl solution at different temperature (293-323)K was studied. The effect of adding different nanomaterial compound (TiO_2 and ZnO (bulk-nano)) is represented in Fig. 3. The corrosion current density (I_{corr}) was calculated by the extrapolation of anodic and cathodic Tafel lines. Table 1 represents the effect of polymer coating with and without nanomaterial on the corrosion parameters of S-steel electrode in 0.2M HCl solution. These parameters are anodic Tafel slope (b_a), cathodic Tafel slope (b_c), corrosion potential (E_{corr}), corrosion current (I_{corr}), IE, weight and penetration loss. Inhibition efficiency was calculated from corrosion current densities using the following equation (1) [32]:

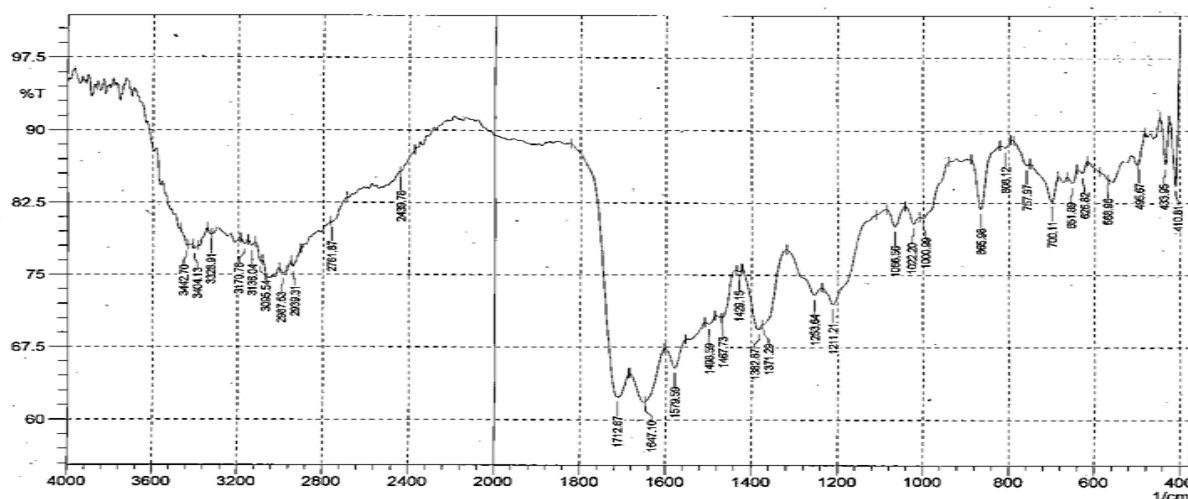


Fig. 2. FTIR spectra of PIM

$$\% I = \left(1 - \frac{i_{corr}}{i_{corr}^0}\right) 100 \quad (1)$$

where i_{corr} and i_{corr}^0 are the corrosion rates of S-steel electrode in the presence and in the absence of coating, respectively.

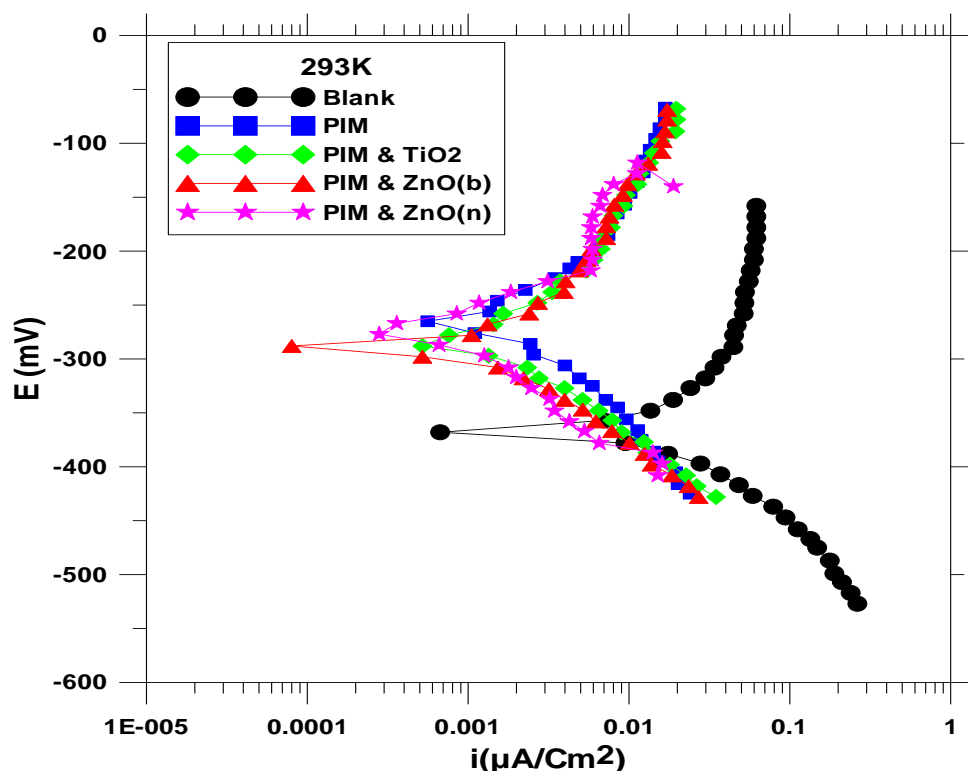


Fig.3. Polarization plots of S-steel coated with polymer and nanomaterial in 0.2M HCl at 293K.

The corrosion potential shifted to more positive values and i_{corr} decreased when the nanomaterial compound adding to the monomer solution indicating the inhibiting effect of these compounds. When the polymer film crafted with nanomaterial coated on the S-steel the corrosion potential shifted to the noble side. This indicates that a film formed on anodic sites of the metal surface [33].

Table 1. Corrosion data of S-steel in 0.2M HCl with and without coating.

| coating | T\K | -E _{corr} mV | i _{corr} μA/cm ² | -b _c mV/Dec | b _a mV/Dec | %I | Weight loss g/m ² .d | Penetration loss[mm/a] |
|----------------------------|-----|-----------------------|--------------------------------------|------------------------|-----------------------|-------|---------------------------------|------------------------|
| Blank 0.2M HCl | 293 | 364.1 | 16.00 | 109.1 | 179.5 | - | 4.01 | 0.178 |
| | 303 | 368.4 | 22.45 | 131.8 | 349.8 | - | 5.63 | 0.25 |
| | 313 | 369.0 | 25.35 | 141.1 | 274.0 | - | 6.35 | 0.283 |
| | 323 | 371.1 | 27.15 | 123.0 | 242.4 | - | 6.81 | 0.303 |
| P.M.I | 293 | 265.9 | 2.65 | 162.8 | 198.5 | 83.43 | 0.664 | 0.0296 |
| | 303 | 272.9 | 3.99 | 165.0 | 153.7 | 82.22 | 1 | 0.0445 |
| | 313 | 291.3 | 5.10 | 223.9 | 330.9 | 79.88 | 1.28 | 0.0569 |
| | 323 | 312.6 | 6.40 | 116.2 | 257.0 | 76.42 | 1.6 | 0.0714 |
| TiO ₂ & P.M.IMD | 293 | 282.1 | 1.64 | 113.1 | 140.9 | 89.75 | 0.412 | 0.0183 |
| | 303 | 290.1 | 2.48 | 114.1 | 118.1 | 88.95 | 0.622 | 0.0277 |
| | 313 | 326.8 | 3.35 | 85.5 | 181.5 | 86.78 | 0.893 | 0.0373 |
| | 323 | 334.5 | 4.59 | 88.3 | 216.6 | 83.09 | 1.15 | 0.0512 |
| ZnO _b &P.M. IMD | 293 | 290.0 | 1.18 | 92.2 | 107.0 | 92.62 | 0.295 | 0.0131 |
| | 303 | 311.2 | 2.00 | 112.3 | 98.6 | 91.09 | 0.502 | 0.0223 |
| | 313 | 313.8 | 2.60 | 124.8 | 186.2 | 89.74 | 0.652 | 0.029 |
| | 323 | 335.5 | 3.72 | 82.7 | 194.3 | 86.29 | 0.934 | 0.0416 |
| ZnO _n &P.M. IMD | 293 | 270.0 | 0.89228 | 128.5 | 76.8 | 94.42 | 0.224 | 0.00995 |
| | 303 | 284.8 | 1.47 | 215.3 | 138.4 | 93.45 | 0.368 | 0.0164 |
| | 313 | 303.8 | 2.17 | 117.3 | 293.9 | 91.43 | 0.543 | 0.0242 |
| | 323 | 335.5 | 3.05 | 68.0 | 71.2 | 88.76 | 0.765 | 0.034 |

3.4. Kinetic and thermodynamic of activation parameters

The corrosion reaction can be regarded as an Arrhenius-type process, the rate is given by [34]

$$C.R = A \exp(-E_a/RT) \quad (2)$$

$$\log C.R = \log A - E_a/2.303RT \quad (3)$$

Where A is the Arrhenius pre-exponential constant and E_a is the activation corrosion energy for the corrosion process, T is the absolute temperature and R is the universal gas constant. Fig. 4 present the Arrhenius plots of the logarithm of the corrosion current density vs 1/T, for 0.2M HCl, without and with polymer and nanomaterial coating. The E_a values were determined from the slopes of these plots and are calculated and are presented in Table 4. The values of enthalpy of activation ΔH^* and entropy of activation ΔS^* were obtained from Fig. 5 from the transition state Eqn (4 and 5) [35]:

$$C.R = RT/Nh \exp(\Delta S^*/R) \exp(-\Delta H^*/RT) \quad (4)$$

$$\log(C.R/T) = \log R/Nh + \Delta S^*/2.303R - \Delta H^*/2.303RT \quad (5)$$

Where h is the Planck's constant, N is the Avogadro's number. A plot of $\log(CR/T)$ as a function of 1/T was made and straight lines were obtained. ΔH^* and ΔS^* were computed from the slope and intercept respectively from the linear plot and are presented in Table 4.

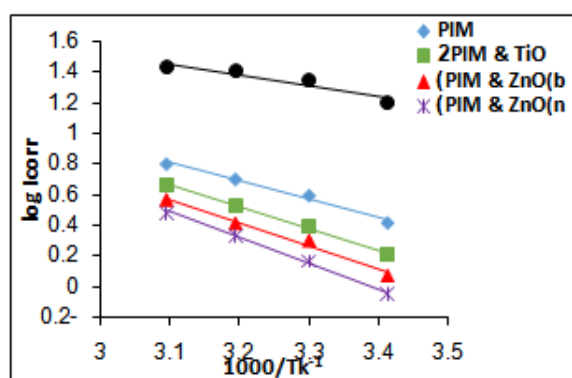


Fig. 4 Arrhenius Plot of log C.R versus 1/T for S-steel in 0.2M HCl in the absence and presence coating.

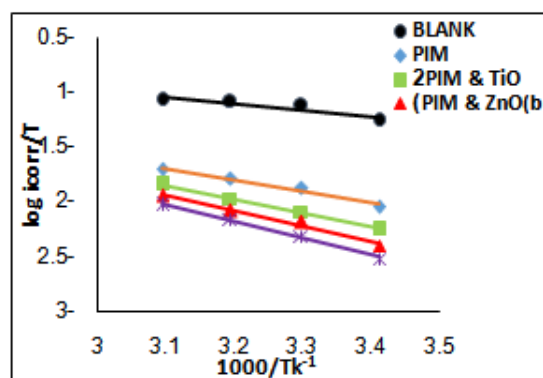


Fig. 5 Arrhenius plots of log C.R/T vs. 1/T for S-steel in 0.2M HCl in the absence and presence

| Coating | R ² | E _a kJ.mol ⁻¹ | A/Molecule. Cm ² .S ⁻¹ | R ² | ΔH* KJ. K ⁻¹ . mol ⁻¹ | -ΔS* J.K ⁻¹ . mol ⁻¹ |
|----------------------|----------------|--|---|----------------|--|---|
| HClBlank | 0.899 | 13.565 | 4.482 x 10 ³ | 0.852 | 11.013 | 183.600 |
| PIM | 0.985 | 22.823 | 3.2337 x 10 ⁴ | 0.981 | 20.271 | 167.172 |
| PIM&TiO ₂ | 0.997 | 26.698 | 9.5962 x 10 ⁴ | 0.996 | 24.144 | 158.127 |
| PIM&ZnO _b | 0.969 | 29.241 | 2.01557 x 10 ⁵ | 0.982 | 26.683 | 151.967 |
| PIM&ZnO _n | 0.991 | 32.13 | 4.89778 x 10 ⁵ | 0.995 | 29.584 | 144.549 |

The inhibition efficiency of coating decreases with temperature increase and its decrease leads to increase the apparent activation corrosion energy. The positive sign of the ΔH^* reflects the endothermic nature of the S-steel dissolution process in the presence and absence of the coating film, while the negative sign of ΔS^* shows an increase in the system order [36-37].

3.5. Antibacterial study

nanotechnology has become increasingly important in the biomedical and pharmaceutical areas as alternative antimicrobial strategy due to reemergence infectious diseases and the appearance of antibiotic resistant strains [38]. Nanoparticles (NPs) are biocidal effectiveness is suggested to be owing to a combination of their small size and high surface to volume ratio, which enable intimate interactions with microbial membranes [39]. The results of antibacterial activity of polymer and polymer with nanomaterial are listed in table 3. The result refer that the polymer and polymer with nanomaterial compounds possess strong activity against *Staphylococcus aureus* and *Escherichia coli*. Among these metal oxides, ZnO has attracted a special attention as antibacterial agent. For instance, ZnO inhibits the adhesion and internalization of *Staphylococcus aureus* and *Escherichia coli* [40].

Table 3. Antimicrobial activity of the tested polymer and polymer with nanomaterial

| compound | <i>Staph.Aure</i> | <i>E. Coli</i> |
|--------------------------|-------------------|----------------|
| PIM | 16 | 12 |
| PIM & TiO ₂ | 17 | 16 |
| PIM & ZnO _(B) | 23 | 25 |
| PIM & ZnO _(n) | 24 | 30 |

Solvent: DMSO; [C]: 800µg/ml.

IV. Conclusion

Electro polymerization of NIM on S-steel surface was found to inhibit the corrosion rate in 0.2M HCl solution. The inhibition efficiency of polymer will increase with adding nanomaterial to monomer solution especially with ZnO(n), and decreases with temperature increase (293-323)K. Beside the resistance to corrosion, polymer coating can also provide antimicrobial activity against *Staphylococcus aureus* and *Escherichia coli* bacteria. With the further studies of Electro polymerization technique and related characterization technologies, Electro polymerization protective coatings will have wider and more practical applications.

References

- [1]. Murray, R.W., Ewing, A.G., Durst, R.A. **1987**. Chemically Modified Electrodes Molecular design for electroanalysis, in *Electroanalytical Chemistry*, 59(5), pp:379–390.
- [2]. Hillman, A.R., Mallen, E. **1987**. Nucleation and growth of polythiophene films on gold electrodes, *J. Electroanal. Chem.*, 220(2), pp:351-367.
- [3]. Hillman, A.R., Mallen, E. **1988**. A spectroelectrochemical study of the electrodeposition of polythiophene films, *J. Electroanal. Chem.*, 243(2), pp:401-417.
- [4]. Roncali, J. **1992**. Conjugated poly(thiophenes): synthesis, functionalization, and applications, *Chem. Rev.*, 92(4), pp:711-738.
- [5]. Desbene-Monvernay, A., Lacaze, P.C., Dubois, J.E. **1983**. Polymer-modified electrodes as electrochromic material: Part IV. Spectroelectrochemical properties of poly-N-vinylcarbazole films, *J. Electroanal. Chem.*, 152(1-2), pp:87-96.
- [6]. Cosnier, S., Deronzier, A., Moulet, J.C. **1985**. Oxidative electropolymerization of polypyridinyl complexes of ruthenium(II)-containing pyrrole groups, *J. Electroanal. Chem.*, 193(1-2), pp:193-204.
- [7]. Burke, D.L., Scannell, R. **1984**. An investigation of hydrous oxide growth on iridium in base, *J. Electroanal. Chem.*, 175(1-2), pp:119-141.
- [8]. Otero, T.F., Larrocha, M.S. **1983**. *Passivity of Metals and Semiconductors*, 1st ed., Elsevier, Amsterdam, p. 725
- [9]. Tsubokawa, N., Takeda, N., Kanamaru, A. **1980**. The Cationic Polymerization Of Carbon Black Surface N-Vinyl-2-Pyrrolidone Initiated, *J. Polym. Sci. Polym. Lett. Ed.*, 18(9), pp:625-628.
- [10]. Tsubokawa, N., Maruyama, H., Sone, Y. **1988**. Cationic Polymerization of N-Vinylcarbazole and N-Vinyl-2-Pyrrolidone Initiated By Carboxyl Groups on Carbon Fibers, *J. Macromol. Sci.-Chem.*, A25(2), pp:171-182.
- [11]. Tsubokawa, N., Yoshihara, T. **1991**. Carbon Whisker as an Initiator of Cationic Polymerization of N-Vinylcarbazole and N-Vinyl-2-pyrrolidone, *Polym. J.*, 23(3), pp:177-183.
- [12]. Haaf, F., Sanner, A., Straub, F. **1985**. Polymers of N-Vinylpyrrolidone: Synthesis, Characterization and Uses, *Polym. J.*, 17(1), pp:143-152.
- [13]. Younang, E., Léonard-Stibbe, E., Viel, P., Defranceschi, M., Lécayon, G., Delhalle J. **1992**. Prospective theoretical and experimental study towards electrochemically grafted poly (N-vinyl-2-pyrrolidone) films on metallic surfaces, *Molec. Engin.* 1(4), pp:317-332.
- [14]. El-Etre, A.Y., El-Tantawy Z. **2006**. Inhibition of metallic corrosion using Ficus extract, *Portugaliae Electrochimica Acta*, 24(3), pp:347–356.
- [15]. Oguzie, E.E., Ebenso, E.E. **2006**. Studies on the corrosion inhibiting effect of Congo red dye – halide mixtures, *Pigment & Resin Tech.* 35(1), pp:30–35.
- [16]. Oguzie, E.E. **2006**. Adsorption and corrosion inhibitive properties of Azadirachta indica in acid solution, *Pigment & Resin Tech.* 35(6), pp:334–340.
- [17]. Bouklah, M., Hammouti, B. **2006**. Thermodynamic characterization of steel corrosion for the corrosion inhibition of steel in sulphuric acid solutions by Artemisia, *Portugaliae Electrochimica Acta*. 24(4), pp:457–468.
- [18]. Firyal, M.A., Khudheyr, J.K., Firas A.R., Estabrak W.G. **2014**. Preparation of Poly (N- Imidazolylmaleamic acid), 17(1), pp:1-6.
- [19]. Younang, E., Léonard-Stibbe, E., Viel, P., Defranceschi, M., Lécayon, G., Delhalle J. **1992**. Prospective theoretical and experimental study towards electrochemically grafted poly (N-vinyl-2-pyrrolidone) films on metallic surfaces, *Molec. Engin.* 1(4), pp:317-332.
- [20]. Léonard-Stibbe, E., Lécayon, G., Deniau, G., Viel, P., Defranceschi, M., Legeay, G., Delhalle J. **1994**. The cationic polymerization of N-vinyl-2-pyrrolidone initiated electrochemically by anodic polarization on a Pt surface, *J. Polym. Sci.: Part A, Polym. Chem.*, 32(8), pp:1551-1555.
- [21]. Je'ro'me, R.; Mertens, M., Martinot, **1995**. On The Electrochemical Polymerization of Acrylonitrile and N-Vinylpyrrolidone - New Insight into the Mechanism, *L. Adv. Mater.*, 7(9), pp:807-809.
- [22]. Beamson, G.; Briggs, D. **1992**. *High Resolution XPS of Organic Polymers*, John Wiley & Sons: Chichester, p 192.
- [23]. Ivanov, D.V., Yelon, **1996**. Chemical-Sensitivity of the Thickness-Shear-Mode Quartz-Resonator Nanobalance, *A. J. Electrochem. Soc.*, 143(9), pp:2835-2841.
- [24]. Czerwinski, W. K., Makromol. **1991**. Solvent effects on free-radical polymerization, 2. IR and NMR spectroscopic analysis of monomer mixtures of methyl methacrylate and N-vinyl-2-pyrrolidone in bulk and in model solvents, *Chem.*, 192(6), pp:1297-1305.
- [25]. Lin-Vien, D., Colthup, N. B., Fateley, W. G., Grasselli, J. G. **1991**. The Handbook of Infrared and Raman Characteristic Frequencies of Organic Molecules, *Academic: San Diego*, p 74.
- [26]. Mertens, M., Calberg, C., Martinot, L., Je'ro'me, R. **1996**. The Electroreduction of Acrylonitrile - A New Insight into the Mechanism, *Macromolecules*, 29(14), pp:4910-4918.

- [27]. Raynaud, M., Reynaud, C., Ellinger, Y., Hennico, G., Delhalle, J. **1990**. High Electric-Field Effects on the Acrylonitrile Molecule - an Abinitio Study, *J. Chem. Phys.*, 142(2), pp:191-201.
- [28]. Geskin, V.M., Lazzaroni, R., Mertens, M., Je'ro'me, R., Bre'das, J. L. **1996**. Acrylonitrile on Cu(100): A density functional theoretical study of adsorption and electrochemical grafting, *J. Chem. Phys.*, 105(8), pp:3278-3289.
- [29]. Silverstein R.M., Webster, F.X., Kiemle, D.J. **1963**. *Spectrometric Identification of Organic Compounds*, 7th ed., John Wiley & Sons, Westford, US.
- [30]. Shirner, R., Fuson, R., Cartin, D., Mrril, T. **1980**. *The systematic identification of organic compound*, 8th ed., John Wiley & Sons, New York.
- [31]. Koj, N., **1962**. *Infrared abstraction spectroscopy*, 1st ed., NankodoCmpany Limited, Tokyo.
- [32]. Seung-Hyun, Y., Young-Wun, K., Kunwoo, C., Seung-Yeop B., Joon-Seop K. **212**. Synthesis and corrosion inhibition behavior of imidazoline derivatives based on vegetable oil, *Corrosion Science*, 59(18), pp:42-54.
- [33]. Anthony, S.S.R., Susai, R. **2012**. Inhibition of corrosion of carbon steel in well water by arginine- Zn^{2+} system, *J. Electrochem. Sci. Eng.* 2(2), pp:91-104.
- [34]. Bentiss, F., Traisnel, M., Chaibi, N., Mernari, B., Vezin, H., Lagrenee, M. **2002**. 2,5-Bis(n-methoxyphenyl)-1,3,4-oxadiazoles used as corrosion inhibitors in acidic media: correlation between inhibition efficiency and chemical structure, *Corrosion Science*, 44(10), pp:2271-2289.
- [35]. Umorena, S.A., Obota, I.B., Ebensob, E.E., Obi-Egbedi, N.O. **2009**. The Inhibition of aluminium corrosion in hydrochloric acid solution by exudate gum from Raphia hookeri, *Desalination*, 247(1-3), pp:561-572.
- [36]. El-Etre, A.Y. **2003**. Inhibition of aluminium corrosion using opuntia extract, *Corros. Sci.* 45(11), pp:2485-2495.
- [37]. Ambrish, S., Ishtiaque, A., Mumtaz, A.Q. **2016**. Piper longum extract as green corrosion inhibitor for aluminium in NaOH solution, *Arabian Journal of Chemistry*, 9(2), pp:S1584-S1589.
- [38]. Desselberger, U., **2000**. Emerging and re-emerging infectious diseases. *J. Infect.* 40(1), pp:3-15.
- [39]. Allaker, R.P., **2010**. The use of nanoparticles to control oral biofilm formation. *J. Dent. Res.* 89(11), pp:1175-1186.
- [40]. Roselli, M., Finamore, A., Garaguso, I., Britti, M.S., Mengheri, E., **2003**. Zinc oxide protects cultured enterocytes from the damage induced by E. coli. *J. Nutr.* 133(12), pp:4077-4082.

Khlood A. Saleh "Preparation of poly (N-imidazolylmaleamic acid) /nanomaterial coating films on stainless steel by electrochemical polymerization to study the anticorrosion and antibacterial action." *IOSR Journal of Pharmacy and Biological Sciences (IOSR-JPBS)* 13.1 (2018): pp 30-36.